JOURNAL OF MATERIALS SCIENCE 32 (1997) 513–522

Tetragonal to monoclinic transformation and microstructural evolution in ZrO_2–9.7 mol% MgO during cyclic heating and cooling

FUJIO ABE, SEIICHI MUNEKI, KOICHI YAGI
National Research Institute for Metals, 1-2-1 Sengen, Tsukuba 305, Japan

The tetragonal (t) to monoclinic (m) transformation behaviour and its relationship to microstructural evolution were investigated by means of dilatometry and transmission electron microscopy for ZrO_2–9.7 mol% MgO during cyclic heating and cooling between room temperature and 1490 K. In the as-sintered specimens, fine oblate ellipsoidal t-phase precipitates, 20–50 nm in diameter and 100–200 nm long, were distributed in the cubic (c)-phase matrix. They were below a critical size for transformation and exhibited no transformation in the first three cycles. In the fourth and further cycles, transformation occurred in two distinct stages. A low-temperature stage appeared at 850–1000 K on heating and at 400–700 K on cooling, while a high-temperature stage appeared at 1350–1400 K on heating and at 1000–1200 K on cooling. With the increasing number of cycles, at first the size of low-temperature stages increased and then decreased above ten cycles accompanying the development of the high-temperature stage. During cyclic heating and cooling, coarsening of ellipsoidal precipitates and decomposition of c- and t-phases occurred. As a result of the decomposition, MgO particles and a new m-phase containing a very low concentration of MgO were produced. The coarsened ellipsoidal t-phase precipitates were responsible for the low-temperature stage. The new m- or t-phase containing very low MgO produced by the decomposition was responsible for the high-temperature stage.

1. Introduction

Transformation-toughened ZrO_2 base ceramics have been of much interest in recent years, because of the considerable potential of these ceramics in structural applications [1]. Pure ZrO_2 has three polymorphs: cubic (c) above 2633 K (2360 °C), tetragonal (t) between 2633 (2360) and about 1473 K (1200 °C), and monoclinic (m) below about 1373 K (1100 °C). The addition of small amounts of Y_2O_3, MgO or CaO stabilizers to ZrO_2 retains the high-temperature phases, the c- and t-phases, at room temperature in metastable states. The ZrO_2 alloys that are a mixture of the c- and m- (or t-) phases are called partially stabilized zirconias (PSZs), such as MgO–PSZ and CaO–PSZ. Stress-induced martensitic transformation from the t- to the m-phase near a propagating crack tip is responsible for the high fracture toughness of PSZ. Therefore, the retention of a metastable t-phase is a primary requirement for transformation toughening of PSZ. The retention can be controlled by several microstructural and chemical factors, such as grain size, tetragonal particle size and concentration of stabilizers.

Compositions of commercial MgO–PSZ occur in the range 8–10 mol % MgO (see Fig. 1 in [2]), in which t-phases appear as small ellipsoidal-shaped precipitates in a c-phase matrix after appropriate sintering [1]. Microstructural evolution and its effects on mechanical properties have been studied by many researchers [3–8] during isothermal annealing at high temperatures and during controlled cooling after sintering. Hannink [8] examined the coarsening process of the ellipsoidal t-phase precipitates for a ZrO_2–9.7 mol % MgO during isothermal annealing at 1693 K (1420 °C), above the eutectoid temperature of 1673 K (1400 °C), and showed that the precipitates optimally aged for mechanical properties had a mean diameter of about 180 nm and a thickness of about 40 nm. Farmer *et al.* [7] studied eutectoid decomposition of the c-phase for ZrO_2 alloys containing 8.1 to 18.6 mol % MgO during isothermal annealing at temperatures below the eutectoid temperature. They observed that diffusional eutectoid decomposition proceeded readily as a cellular reaction for several hours at 1373–1473 K. However, the relationship between microstructure and t–m transformation behaviour has scarcely been investigated [9, 10]. It is considered that the t–m transformation temperature during heating and cooling is directly related to the thermal stabilities of the t- and m-phases. Hannink and Swain [9] studied thermal dilatation behaviour for a ZrO_2–9.7 mol % MgO in the range between

0022–2461

room temperature and ~ 1473 K after a variety of ageing treatments at 1693 and 1373 K. They observed that the dilatation behaviour, reflecting transformation behaviour, was affected significantly by the ageing treatments and also pointed out the importance of thermal history. But a systematic explanation for the microstructure and t–m transformation relationship was not provided. Dworak *et al.* [10] studied the dilatation behaviour for two grades of ZrO_2–9.2 mol% MgO during cyclic or repeated heating and cooling in the range between room temperature and 1173 K. The specimen with a high m-phase content, 0.2–0.3 in volume fraction, exhibited a hysteresis effect in the dilatation curves, which arose from the t–m transformation. The transformation temperature did not change with repeated cyclic heating and cooling, indicating that microstructural factors determining the transformation temperature did not change during heating and cooling. However, microstructural evolution will occur, as can be expected by earlier results [3–8], if the specimen is heated to temperatures $\geqslant 1373$ K. Microstructural evolution resulting from eutectoid decomposition of the c-phase is more readily controlled for MgO–PSZ than for CaO–PSZ, because the diffusion rates of Mg ions in the ZrO_2 lattice are much larger than those of Ca ions [11] and the eutectoid temperature is higher in ZrO_2–MgO (1673 K) than in ZrO_2–CaO (1413 K) [12]. Extremely long times are required for the occurrence of eutectoid decomposition in CaO–PSZ at temperatures below the eutectoid temperature.

The purpose of the present research is to investigate the microstructure and t–m transformation relationship by means of dilatometry and transmission electron microscopy for a ZrO_2–9.7 mol% MgO during cyclic heating and cooling. The cyclic and cooling experiments were repeated up to 68 cycles over a range between room temperature and 1490 K. The transformation takes place in two distinct stages, i.e. in low- and high-temperature stages. During heating and cooling, coarsening of ellipsoidal t-phase precipitates and decomposition of c- and t-phases occur. The transformation behaviour is discussed taking into account the evolution of the diffusional microstructural during cyclic annealing.

2. Experimental procedure

Sintered bars of partially stabilized zirconia containing 9 mol% MgO (nominal) were used in this study. The main impurities were 20 SiO_2, 50 Fe_2O_3 and 100 (wt p.p.m.) Na_2O. The concentrations of MgO in the specimens were analysed by electron probe microanalysis (EPMA) to be 9.7 mol%. Sintering was carried out at 1973 K, followed by slow cooling to room temperature. According to the equilibrium phase diagram of the ZrO_2–MgO system [2], the ZrO_2–9.7 mol% MgO alloy consists substantially of c-phases at the sintering temperature, 1973 K. After sintering, the specimens pass through the c + t, t + MgO and then M + MgO regions during cooling to room temperature.

The specimens were subjected to heating and cooling in a dilatometer (TD-5020, MAC Science Corporation, Japan) in a range between room temperature and 1490 K. In this temperature range, the thermodynamically stable phases are MgO and the m-phase containing quite low contents of MgO. The dimensions of the specimens were $3 \times 4 \times 18$ mm. Both heating and cooling rates were controlled at $0.17\ \mathrm{K\,s^{-1}}$ ($10\ \mathrm{K\,min^{-1}}$). Differential dilatation between the specimen and an Al_2O_3 bar was measured during heating and cooling. The sensitivity of the differential dilatation measurement was 0.1 μm. To obtain the dilatation of the specimen, the dilatation of the Al_2O_3 bar was subtracted from the measured differential dilatation, assuming the coefficient of thermal expansion of Al_2O_3 to be $8.8 \times 10^{-6}\ \mathrm{K^{-1}}$ [13]. The constituent phases were identified on 0.5 mm thick sheet specimens taken from bars using a low speed diamond saw, by X-ray diffraction (Jeol 3500) using CuK_α radiation (wavelength, $\lambda = 0.154\,05$ nm). Microstructural observations were metallographically carried out using transmission electron microscopy (TEM, JEM 2010) at 200 kV. The distributions of Mg-ions in the specimens were analysed by energy dispersive X-ray (EDX) spectroscopy in the TEM under diffraction conditions. Thin foils for TEM observations were cut from the bars, mechanically polished and thinned to perforation using conventional ion-milling techniques.

3. Results

3.1. Microstructure in the as-sintered condition

The constituent phases in the as-sintered specimens were the t- and c-phases, with small amounts of m-phase, as shown in Fig. 1. Any peaks from MgO could not be detected in the 2θ range between 25 and 80°. For MgO, having an NaCl type structure with a lattice parameter of 0.421 nm [7], a maximum diffraction peak should appear from the (200) plane at $2\theta = 43.9°$ under CuK_α radiation. The $(1\,1\,1)_t$ and $(1\,1\,1)_c$ peaks overlap each other because they have nearly the same lattice parameters for the t- and c-phases. The volume fraction of the m-phase was estimated to be 0.19, using an expression proposed by Porter and Heuer [3] as

$$V_m = 1.603[I(1\,1\,1)_m]/\{1.603[I(1\,1\,1)_m] + I(1\,1\,1)_{c,t}\} \quad (1)$$

where $I(1\,1\,1)_m$ and $I(1\,1\,1)_{c,t}$ are the integrated intensities of the $(1\,1\,1)_m$ and $I(1\,1\,1)_{c,t}$ peaks. The volume fractions of the t- and c-phases were evaluated by peak-separation of the high-angle $(4\,0\,0)_{t,c}$ peaks by the least squares method. This is shown in Fig. 2. We obtained $V_t/V_c = [I(4\,0\,0)_t + I(0\,0\,4)_t]/I(4\,0\,0)_c = 1.49$. Then the volume fractions of the t-, c- and m-phases in the as-sintered specimens are estimated to be 0.48, 0.33 and 0.19, respectively.

The t-phases in the as-sintered specimen were observed to be fine oblate ellipsoidal precipitates 20–50 nm in diameter and 100–200 nm long. The

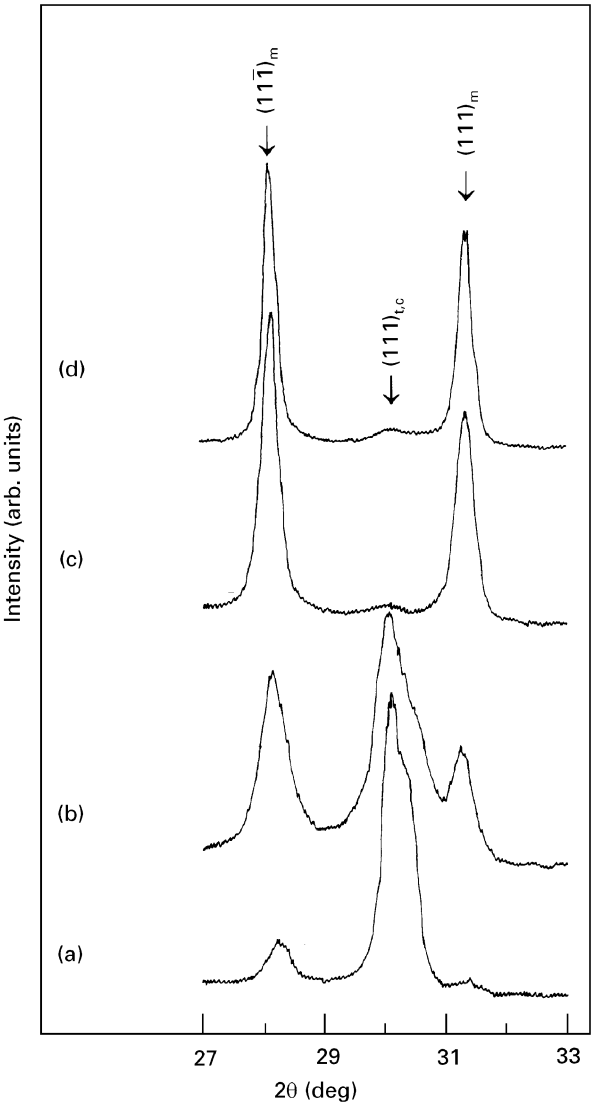

Figure 1 X-ray diffraction patterns of the $(1\,1\,1)_m$, $(1\,1\,1)_{t,c}$ and $(1\,1\,\bar{1})_m$ peaks of (a) the as-sintered specimen, and for specimens after (b), seven and (c) 68 cycles of heating and cooling, and (d) following heating at 1373 K and annealing for 40 h. The $(1\,1\,\bar{1})_m$ peak is a maximum peak from the m-phase. The $(1\,1\,1)_t$ and $(1\,1\,1)_c$ peaks, which are maximum peaks from the t- and c-phases, overlap each other.

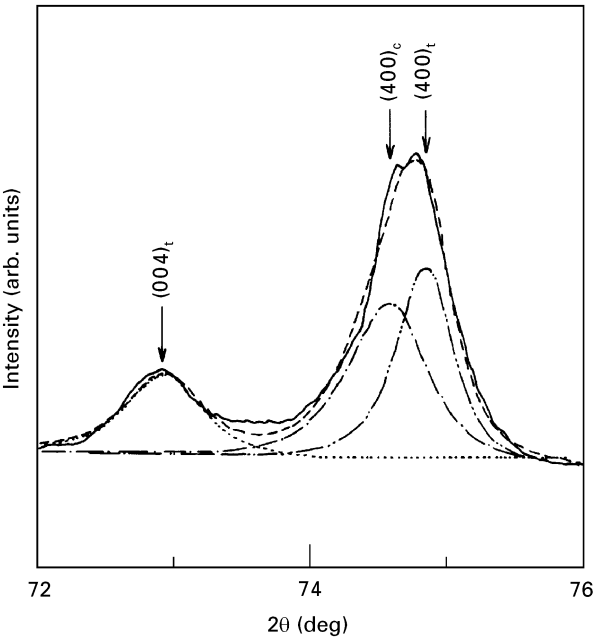

Figure 2 Peak-separation of $(400)_{t,c}$ diffraction peak for the as-sintered ZrO_2–9.7 mol% MgO specimen. (–) results; (----) $(004)_t$; (–·–·) $(400)_c$; (–··–) $(400)_t$; (– – –) sum of $(004)_t$, $(400)_c$ and $(400)_t$.

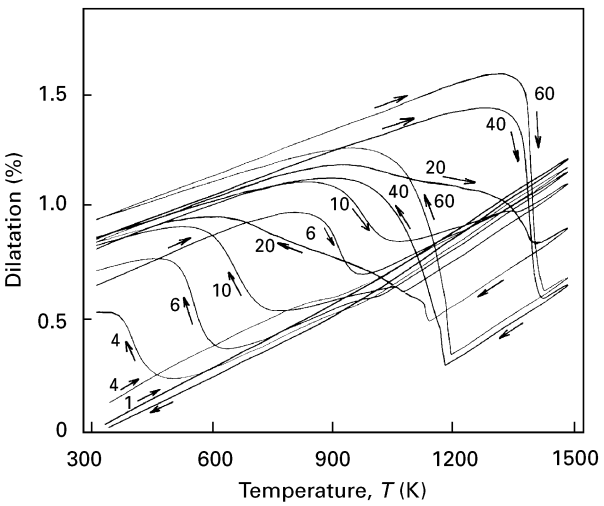

Figure 3 Dilatation–temperature curves of the ZrO_2–9.7 mol% MgO specimen during cyclic heating and cooling at a rate of 10 K min^{-1}. The numbers refer to the number of cycles.

oblate ellipsoidal precipitates were densely distributed in the three mutually orthogonal [100] orientations in the (100) plane of the c-phase matrix, which was the same as in earlier results [1]. During observation, some of the ellipsoidal t-phase precipitates transformed to m-phases having substructures comprising parallel variants where adjacent pairs were twin related. The variants extended either parallel or normal to the axes of rotation of the ellipsoidal precipitates as observed by Muddle and Hannink [5]. It is likely that the transformations occurred with the aid of local stress during electron beam irradiation in the TEM.

3.2. Kinetics of tetragonal–monoclinic phase transformation

Fig. 3 shows the dilatation–temperature curves of the specimen during cyclic heating and cooling. In this figure, only the results of cycles 1, 4, 6, 10, 20, 40 and 60 are shown for simplicity, although cyclic annealing was carried out for up to 68 cycles using one specimen. In the first three cycles, the dilatation behaviour was identical with that of the first cycle where virtually no inflection occurred in the dilatation curve, indicating no transformation. This suggests that the ellipsoidal t-phase precipitates in the as-sintered specimen are below a critical size for transformation to m-phases above room temperature. Hannink and Swain [9] already observed for their ZrO_2–9.7 mol% MgO alloy that virtually no transformation occurred in the as-sintered condition. The average thermal expansion coefficient of the specimen was evaluated from the dilatation curve at the first cycle to be 10.0×10^{-6} K^{-1} which is the same as that of polycrystalline

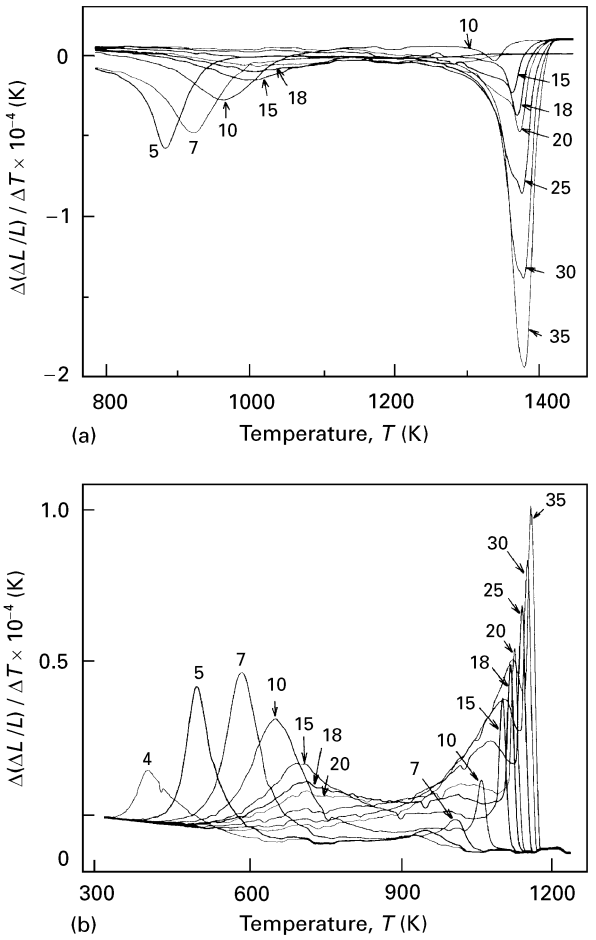

Figure 4 Temperature derivative curves of the dilatation curves during (a) heating and (b) cooling for ZrO_2–9.7 mol% MgO at a rate of 0.17 K s^{-1}. The numbers refer to the number of cycles.

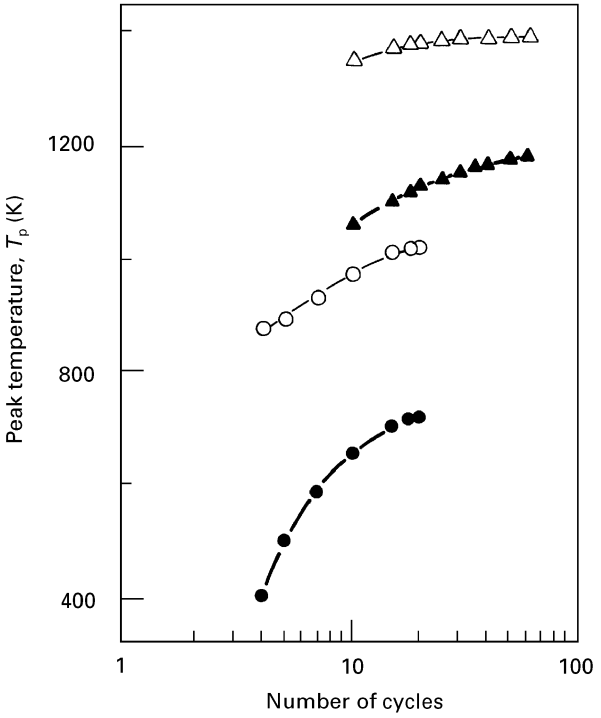

Figure 5 Peak temperature in the derivative curves in Fig. 4, as a function of the number of cycles on heating (○, △) and cooling (●, ▲) at a rate of 0.17 K s^{-1} for H1 (○), H2 (△), C1 (●), and C2 (▲)

ZrO_2–(2–3) mol% Y_2O_3 consisting of t-phases, $(10.0–10.5) \times 10^{-6}$ K^{-1} [14]. In subsequent cyclic annealing above four cycles, inflections appear repeatedly. The inflections exhibiting an increase in length on cooling result from transformation of t-phases to m-phases and those exhibiting a reduction in length on heating result from back-transformation of m-phases to t-phases. The $t \rightarrow m$ transformation on cooling took place at a lower temperature than the m → t transformation on heating, forming hysteresis loops.

Fig. 4a and b shows the temperature derivatives of the dilatation curves in Fig. 3. The derivative curves exhibit peaks at temperatures at which the inflections appear in the dilatation curves, and the peak temperature was defined as temperature of the transformation. The peaks appeared at 850–1000 and 1350–1400 K on heating, designated stages H1 and H2, respectively, and at 400–700 and 1000–1200 K on cooling, designated stages C1 and C2, respectively. The present results indicate that the transformation takes place in two distinct stages not in a single stage. The stages H1 and H2 on heating correspond to back-transformation of stages C1 and C2 on cooling, respectively. The low-temperature stages, H1 and C1, were dominant in the low cycle range below about ten and then decreased above about ten cycles. The high-temperature stages, H2 and C2, started to develop after decreasing the low-temperature stages and then became saturated above about 40 cycles. The high-temperature stage, C2, on cooling has a substage at the lower temperature side. The substage developed pronouncedly at about 20–30 cycles but overlap with the main stage, C2, at higher cycles above about 40 cycles. The high temperature stage, H2, on heating has a shoulder at the lower temperature side at around 25 cycles. Hannink and Swain [9] observed inflections in the dilatation–temperature curves at ~900–1000 K on heating and at 500–700 K on cooling for a ZrO_2–9.7 mol% MgO after ageing at 1693 K for 4–8 h or at 1373 K for 8–16 h. Dworak *et al.* [10] observed inflections in the dilatation curves at about 980 K on heating and at about 520 K on cooling for a ZrO_2–9.2 mol% MgO during cyclic heating and cooling between room temperature and 1173 K. The low-temperature stage observed in the present work corresponds to the transformation observed by Hannink and Swain and by Dworak *et al.* Hannink and Swain also briefly stated that a second inflection appeared at about 1473 K after prolonged ageing at either temperature, 1373 or 1673 K, although neither experimental results on the dilatation curves nor ageing conditions were presented in their paper. The second inflection at about 1473 K may correspond to the high-temperature stage in the present work.

Fig. 5 shows the cyclic dependence of the peak temperature in the derivative curves. With increasing number of cycles, the peak temperature in each stage shifts to higher temperatures and then saturates at high cycles above about 40 cycles. The low-temperature stages, H1 and C1, shift from 870 and 400 K, respectively, at four cycles to 1020 and 715 K, respectively, at 20 cycles. The high-temperature stages, H2 and C2, shift from 1350 and 1060 K, respectively, at

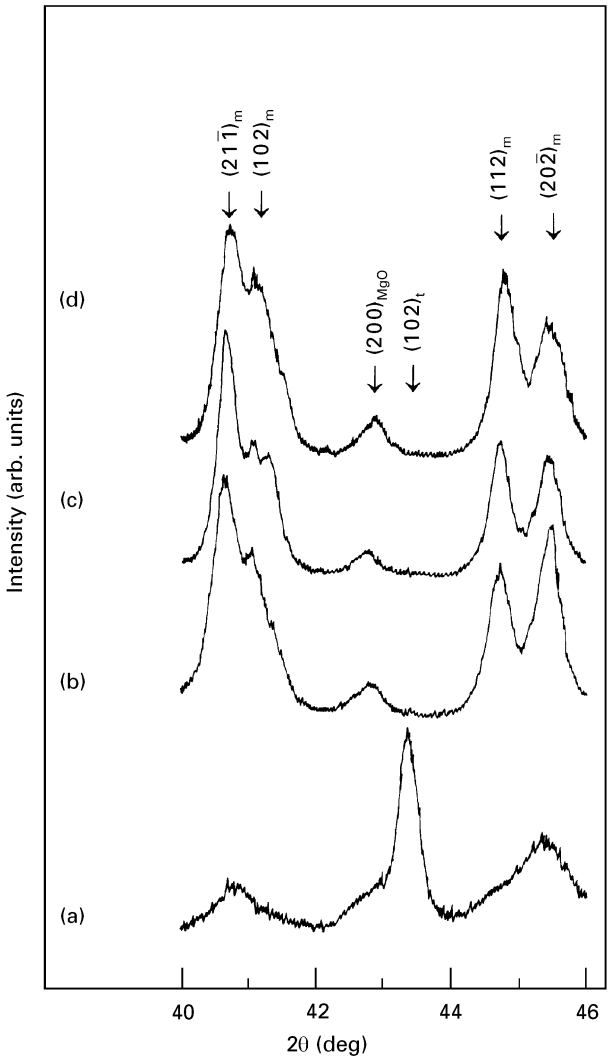

Figure 6 X-ray diffraction patterns of the specimens after various treatments, showing an increase in intensities from the m-phase and MgO and a decrease in intensity from the t-phase compared with those in the as-sintered condition.

ten cycles to 1380 and 1180 K, respectively, at 60 cycles. The peak temperatures of the high-temperature stage at high cycles above 40 are slightly lower than the transformation temperature of pure ZrO_2, about 1400 K on heating and 1273 K on cooling [14].

3.3. Microstructural evolution

With increasing number of cycles, the volume fraction of the m-phase increased but that of the c- and t-phases decreased as shown in Fig. 1. It should be noted that a diffraction peak from the (200) plane of MgO was also observed at $2\theta = 42.9^\circ$ after 68 cycles. This is shown in Fig. 6. The specimen consisted substantially of the m-phase and MgO after 68 cycles. Any MgO peaks were not observed in the as-sintered and after seven cycle specimens.

Fig. 7a shows the microstructure of the specimen after seven cycles at which the low-temperature stage was dominant as shown in Figs. 3 and 4. Transformation-induced microcracks, 50–100 nm in length, were observed to have formed in the matrix and along grain boundaries, although the density of the microcracks

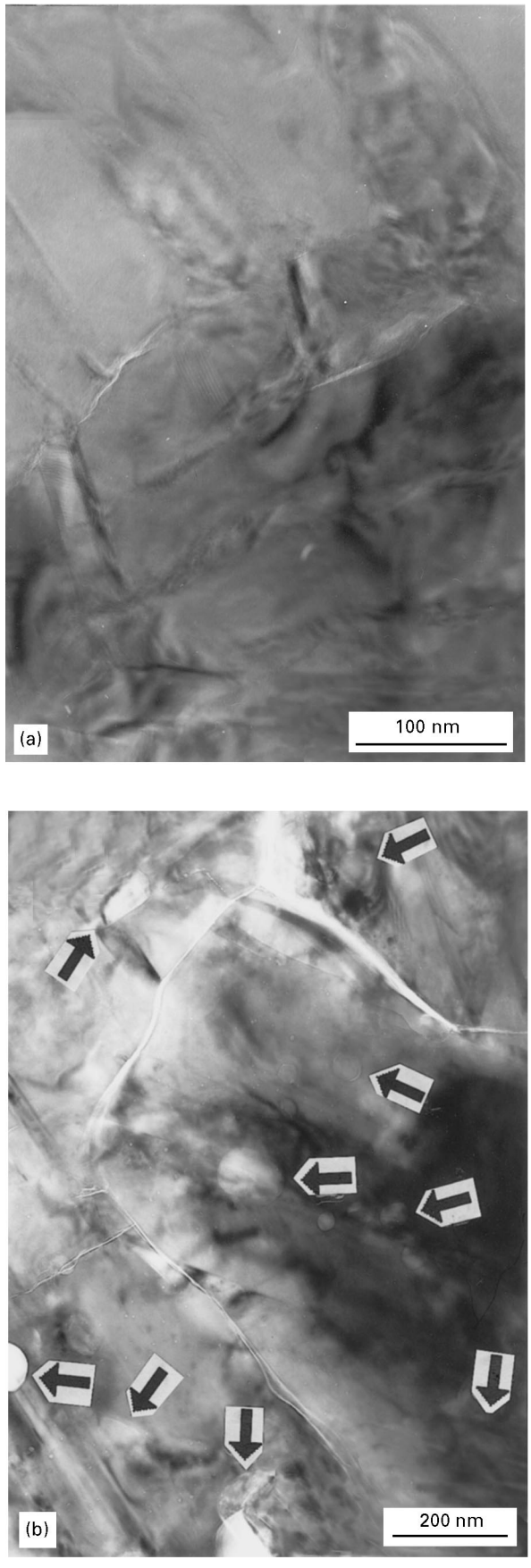

Figure 7 TEM micrographs of the specimens after (a) seven and (b) 68 cycles. The arrows show the MgO particles.

was very low. Orthogonal distributions of the ellipsoidal t-phase precipitates in the c-phase matrix were still observed, similar to those in the as-sintered specimen. The ellipsoidal precipitates have grown to

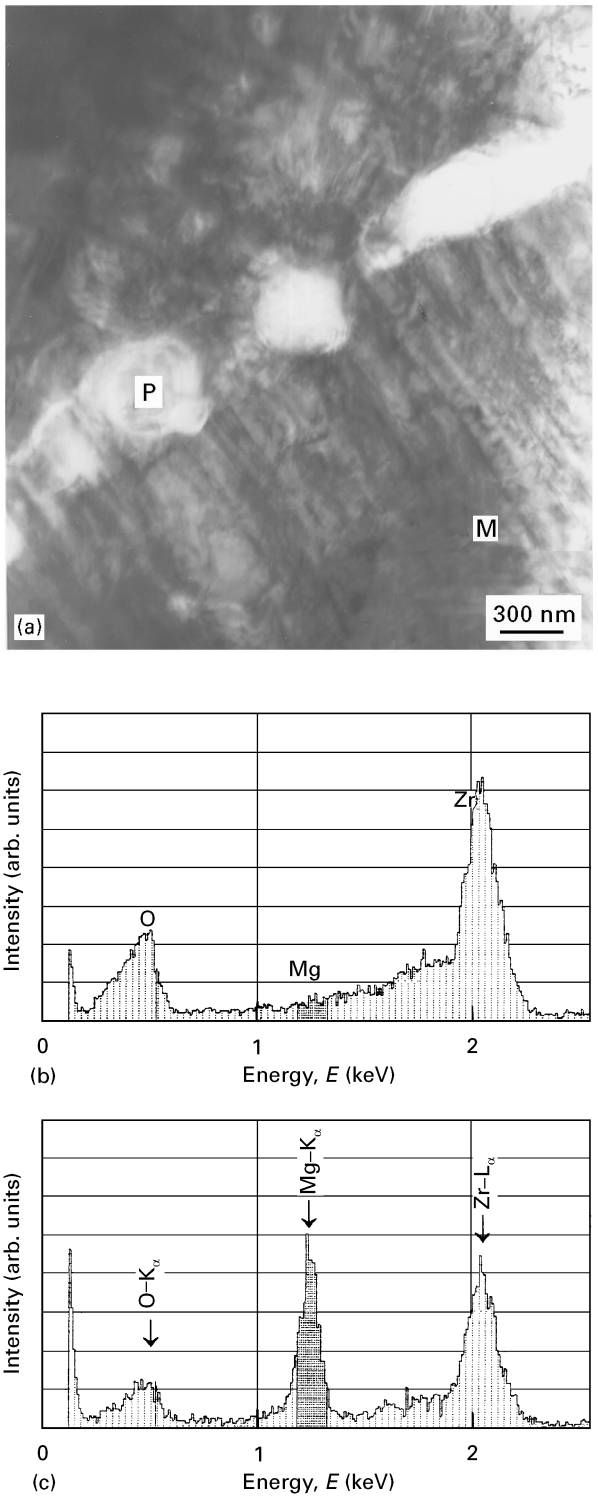

Figure 8 TEM micrograph of matrix (M) and precipitate (P) and (b, c) a set of EDX spectra for the specimen after 68 annealing cycles ∅ for the matrix (b) and precipitate (c).

60–70 nm in diameter and 200–300 nm in length; compared with 20–50 nm in diameter and 100–200 nm in length in the as-sintered condition. With the increasing number of cycles, the number and size of microcracks increased. After 68 cycles, a large number of microcracks was observed to have formed mainly along grain boundaries, as shown in Fig. 7b. The microcracks are considered to be produced as a result of the accommodation of transformation-induced strain. Using the lattice parameters of t- and m-phases in ZrO_2–9.4 mol% MgO [1, 15], which is roughly the same composition as the present alloy, the t → m transformation is accompanied by a volume increase of about 4%. This caused an increase in microcracks with repeated transformation. On the other hand, the formation of MgO particles and rods was also observed in the m-phase matrix. No evidence was found for the formation of MgO in the specimen after seven cycles. Farmer *et al.* [7] observed the formation of rod- and ribbon-shaped MgO in ZrO_2–MgO alloys containing 8.1–18.6 mol% MgO after isothermal annealing at temperatures between 1373 and 1573 K. They also observed that the rod- and ribbon-shaped MgO particles became spheroidal with increasing annealing time.

Fig. 8 shows the bright-field image and Fig. 8b and c a set of EDX spectra taken from the matrix (b) and MgO particles (c) in the specimen after 68 cycles. The peaks at 0.53, 1.25 and 2.04 keV result from O-8 K_α, Mg-12 K_α and Zr-40 L_α, respectively. The concentration of MgO was evaluated to be about 1–2 mol% in the m-phase matrix and about 50–60 mol% in the region containing the MgO particle. Taking into account that the accuracy of MgO concentration analysis is about 1 mol% and that the MgO particle is embedded in the m-phase matrix, the concentration of MgO in the m-phase matrix is quite low and the MgO particles consist substantially of pure MgO. On the other hand, the concentration of MgO in the as-sintered specimen was analysed to be 8–10 mol%, which was approximately the same as the 9.7 mol% by EPMA result, and was fairly uniform in the specimen. This indicates that there are no compositional differences among the c-, t- and m-phases in the as-sintered specimen. The present results suggest that the c-, t- and m-phases containing 9.7 mol% MgO in the as-sintered specimen decomposed into MgO and a new m-phase containing a very low content of MgO during cyclic heating and cooling. The decomposition products, MgO and a new m-phase containing a very low content of MgO, appear to be consistent with the thermodynamically stable phases anticipated from the phase diagram.

4. Discussion

4.1. Decomposition of c- and t-phases and its effect on the t–m transformation

Farmer *et al.* [7] studied the kinetics of the eutectoid decomposition of the c-phase for ZrO_2 alloys containing 8.1–18.6 mol% MgO during isothermal annealing at temperatures between 1373 and 1573 K for up to 16 h. They found that the rate of eutectoid decomposition was maximum at 1473 K. In this research, in order to investigate the effect of decomposition of the c- and t-phases on the transformation behaviour, dilatation measurement was carried out after completing decomposition by isothermal annealing at 1373 K. X-ray diffraction (Figs 1 and 6) and microstructural observations showed that the decomposition of the c- and t-phases was complete and the specimen substantially consisted of MgO and low-MgO-content m-phase after isothermal annealing for 40 h at 1373 K.

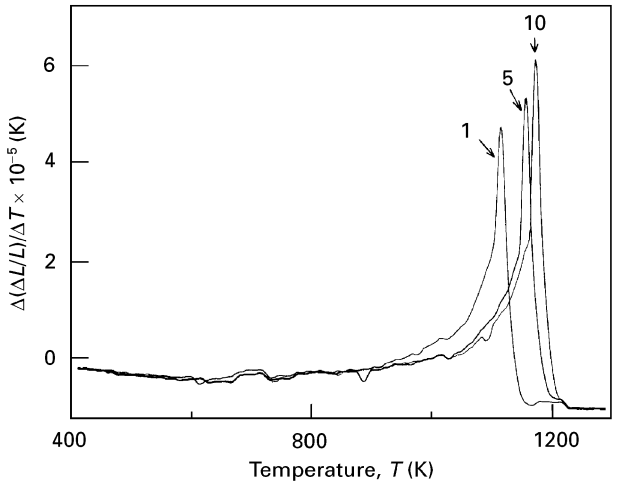

Figure 9 Temperature derivative dilatation curves of the specimen after isothermal annealing at 1373 K for 40 h. Cooling rate = 0.17 K s^{-1}. The numbers refer to the number of cycles.

Fig. 9 shows the temperature derivatives of dilatation for the specimen after isothermal annealing at 1373 K for 40 h, where the results on cooling runs are shown. Cyclic heating and cooling were carried out for up to ten cycles. Only the high-temperature stage, C2, appears, there is no low-temperature stage, C1. This indicates that the decomposition products are responsible for the high-temperature stages. Yoshikawa and Suto [14] reported for ZrO_2–Y_2O_3 alloys that the transformation took place at higher temperatures with decreasing concentration of Y_2O_3 stabilizer. Because the peak temperatures of the high-temperature stage at high cycles above 40 were slightly lower than the transformation temperature of pure ZrO_2 and the MgO particles exhibit no transformation, the high-temperature stages are considered to be caused by a martensitic transformation of the low-MgO-content m- and t-phases that were produced by decomposition of the c- and t-phases.

The following decomposition reactions are considered to take place

c-phase (9.7 mol% MgO) → t- or m-phase

(low MgO) + MgO (2)

t-phase (9.7 mol% MgO) → t- or m-phase

(low MgO) + MgO (3)

Equation 2 represents the eutectoid decomposition of the c-phase. Farmer *et al.* [7] state that the reaction c-phase → m-phase + MgO, the same as Equation 2, dominates the eutectoid decomposition at temperatures below 1473 K, but that another reaction, c-phase → t-phase + MgO, occurs at 1573 K, as expected from the phase diagram shown in Fig. 1. In the present specimens, the eutectoid products appear to be the low-MgO t-phase, rather than the low-MgO m-phase, as will be described later. It should be noted that the decomposition reaction given by Equation 3 also took place, because the original t-phase containing 9.7 mol% MgO in the as-sintered specimens disappeared almost completely. We only detected MgO and the low-MgO-content m-phase, but not the low-MgO-content t-phase by X-ray diffraction and EDX spectroscopy at room temperature after cyclic or isothermal annealing. Even if a low-MgO-content t-phase is produced by decomposition at high temperature, it can easily transform to the m-phase during cooling to room temperature, because of the very low concentration of MgO stabilizer.

4.2. Mean diffusion distance of Mg ions during cyclic heating and cooling

The mean diffusion distance, X_n, of Mg ions in the ZrO_2 lattice during n cycles between a minimum temperature, T_{min}, and a maximum temperature, T_{max}, is given by

$$X_n = \left[\int_0^{\tau} nD_0 \exp(-Q/RT)\,dt\right]^{1/2} = (2nD_0/\alpha)^{1/2}\left[\int_{T_{min}}^{T_{max}} \exp(-Q/RT)\,dT\right]^{1/2} \quad (4)$$

where τ is the total time during one cycle, D_0 the pre-exponential factor of the diffusion coefficient for Mg ions in ZrO_2, Q the activation energy, R the gas constant; and α the heating and cooling rates, given by $\alpha = dT/dt$. As shown in the appendix, Equation 4 can be expressed as [16, 17]

$$X_n \doteqdot (2nR/\alpha Q)^{1/2}[T_{max}D_{max}^{1/2} - T_{min}D_{min}^{1/2}] \quad (5)$$

where D_{max} and D_{min} are the diffusion coefficients $[= D_0 \exp(-Q/RT)]$ at T_{max} and T_{min}, respectively. The term $(T_{min}D_{min}^{1/2})$ is negligibly small compared with the term $(T_{max}D_{max}^{1/2})$ for T_{min} = room temperature and T_{max} = 1490 K. Using $\alpha = 0.17$ K s^{-1} and diffusion data [11] of $D_0 = 5.9 \times 10^{-8}$ m^2 s^{-1} and $Q = 293$ kJ mol^{-1} for Mg ions in cubic ZrO_2, we obtain $X_n = 4.8 \times 10^{-2} n^{1/2}$ (μm) for T_{max} = 1490 K. Fig. 10 shows the mean diffusion distance of Mg ions as a function of the number of cycles. X_n is evaluated to be 1.0×10^{-1} μm for four cycles, from which the low-temperature stage started to develop; 1.5×10^{-1} μm for ten cycles, from which the high-temperature stage started to develop; and to be 3.0×10^{-1} μm for 40 cycles, above which the high-temperature stage saturated. Above ten cycles, X_n is nearly the same as or slightly larger than the mean distance, about 0.2 μm (Fig. 7b), between the MgO particles formed by the decomposition. On the other hand, the mean diffusion distance of Mg ions during isothermal annealing at 1373 K is given by $X = (Dt)^{1/2} = 3.9 \times 10^{-2} t^{1/2}$ (μm), where t is given by hours, using the diffusion data [11]. X is evaluated to be 2.5×10^{-1} μm for 40 h at which decomposition of the c- and t-phases is almost completed. Thus, the mean diffusion distance of Mg ions in ZrO_2 for 40 cycles of heating and cooling between room temperature and 1490 K at a rate of 10 K min^{-1} is approximately the same as that during isothermal annealing at 1373 K for 40 h, at which decomposition of the c- and t-phases is almost completed. It is concluded that enough diffusion of Mg ions takes place in the ZrO_2 lattice for the formation of MgO particles during cyclic or isothermal annealing.

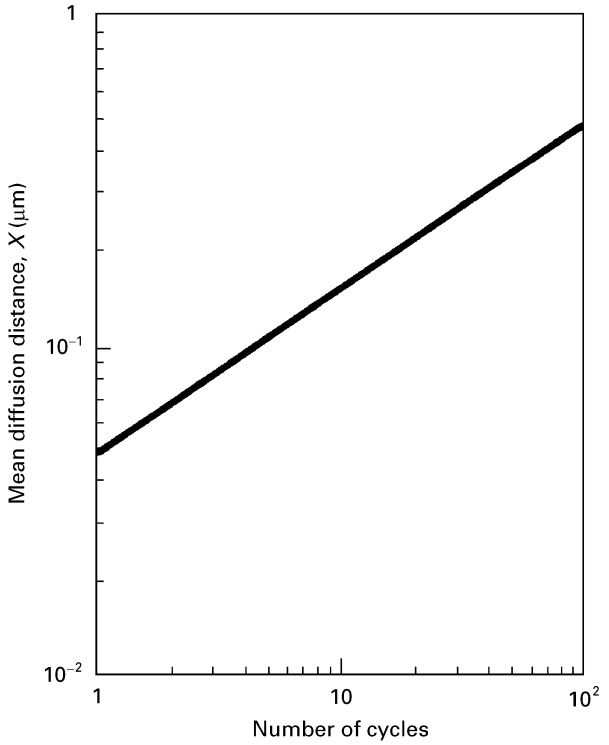

Figure 10 Mean diffusion distance of Mg ions in the ZrO_2 lattice during cyclic heating and cooling between room temperature and $I_{max} = 1490$ K at a rate of 10 K min^{-1}, as a function of the number of cycles. The mean diffusion distance, $X_n = n^{1/2}X_1$, was evaluated using Equation 5.

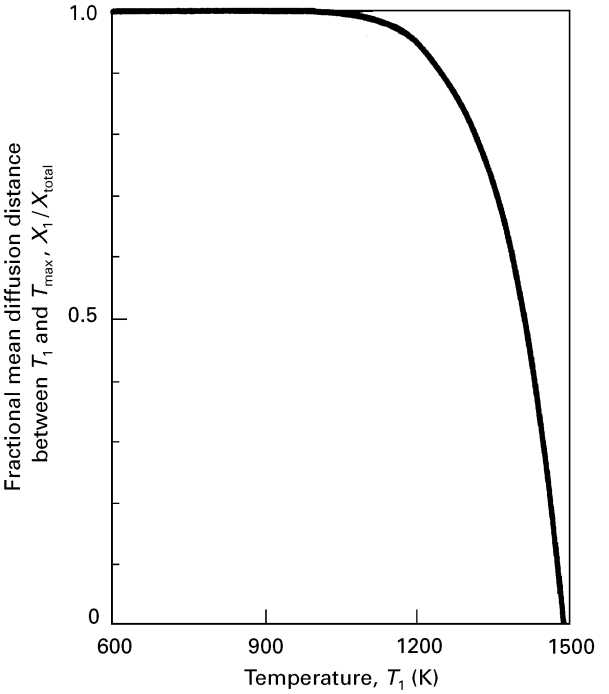

Figure 11 Fractional mean diffusion distance of Mg ions in the temperature range between T_1 and T_{max} (Equation 6), as a function of temperature, T_1.

Dworak *et al.* [10] performed cyclic heating and cooling experiments for a ZrO_2–9.2 mol% MgO up to ten cycles between room temperature and 1173 K at a rate of 5 K min^{-1} and observed only the low-temperature stage; at 980 K on heating and at 520 K on cooling. Using Equation 6, X_n for Mg ions is evaluated to be 7.0×10^{-3} μm for ten cycles. X_n in their specimen is much smaller than the critical value of 1.5×10^{-1} μm for the development of the high-temperature stage described above. It needs about 5×10^3 cycles to reach a critical value of 1.5×10^{-1} μm under their experimental conditions of heating up to 1173 K at a rate of 5 K min^{-1}. On the other hand, Hannink and Swain [9] also observed only the low-temperature stage for a ZrO_2–9.7 mol% MgO after ageing at 1693 K for 4–8 h or at 1373 K for 8–16 h. The mean diffusion distance of Mg ions during ageing is evaluated to be 1.5×10^{-1} μm at 1373 K for 16 h, which just reaches the critical value for the development of the high-temperature stage. Therefore, it is considered that further ageing produces the high-temperature stage. The ageing at 1693 K results in the coarsening of t-phase precipitates but not the eutectoid decomposition, because of the higher ageing temperature above the eutectoid temperature, 1673 K. This causes only the low-temperature stage.

The fractional mean diffusion distance of Mg ions in the temperature range between an intermediate temperature, T_1, and a maximum temperature, T_{max}, to the total mean diffusion distance between room temperature, $T_{r.t.}$, and T_{max} is given by

$$X_1/X_{total} = (T_{max}D_{max}^{1/2} - T_1 D_1^{1/2})/(T_{max}D_{max}^{1/2} - T_{r.t.}D_{r.t.}^{1/2}) \quad (6)$$

and is shown in Fig. 11, as a function of T_1. The fractional mean diffusion distance, X_1/X_{total}, is evaluated to be 0.8 at $T_1 = 1320$ K. This indicates that diffusion of Mg ions for the decomposition reactions, Equations 2 and 3, during heating and cooling substantially takes place in the temperature range between 1320 K and the maximum heating temperature 1490 K. Therefore, diffusion-controlled microstructural evolution, such as the coarsening of ellipsoidal precipitates and decomposition of the c- and t-phases, appears to proceed substantially at high temperatures above ~ 1320 K during cyclic heating and cooling.

4.3. Relationship between microstructural evolution and the t–m transformation

Fig. 12 shows the schematics of the high-temperature and low-temperature stages on the phase diagram. Ellipsoidal t-phase precipitates containing 9.7 mol% MgO in the as-sintered specimens are below a critical size for transformation, but they can grow in size, above the critical size, by diffusion with the increasing number of cycles. This produces the low-temperature stage. The shift of the low-temperature stage to higher temperatures with the increasing number of cycles results from further coarsening of the ellipsoidal precipitates. The temperature of the low-temperature stage is much lower than the thermodynamic equilibrium transformation temperature, 1513 K (1240 °C), in the phase diagram, and is considered to be the transformation temperature for metastable t- and m-phases. Further increase in cyclic annealing causes decomposition of the c- and t-phases containing 9.7 mol% MgO, forming a new m- or t-phase containing 1–2 mol% MgO. The much lower MgO concentration in the new m- or t-phase brings about an extra

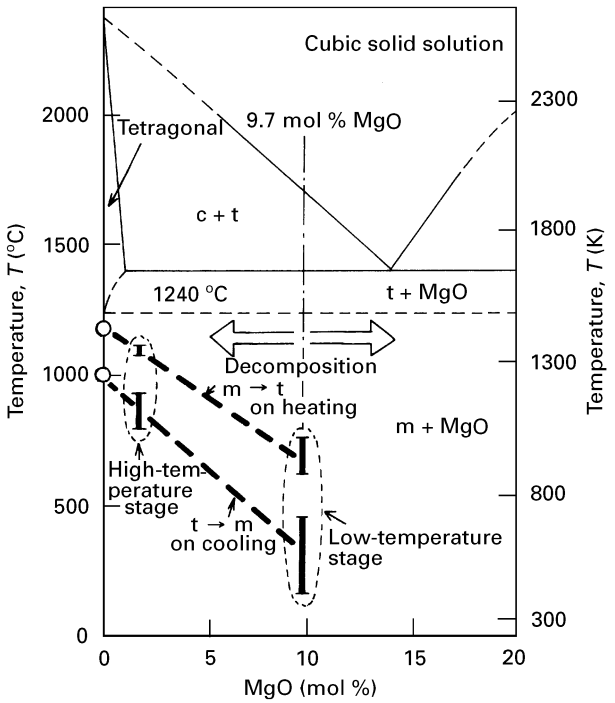

Figure 12 Schematic drawings of the low- and high-temperature stages for the t–m transformation in ZrO_2–9.7 mol% MgO on the phase diagram. The open circles show the transformation temperatures for pure ZrO_2 by Yoshikawa and Suto [14].

stage at temperatures much higher than the low-temperature stage. This produces the high-temperature stage. The thick dotted lines in Fig. 12 represent the dependence of the MgO concentration on the t–m transformation temperatures on heating and cooling, where the low- and high-temperature stages are plotted at 9.7 and 1–2 mol% MgO, respectively. The results on pure ZrO_2, shown by the open circles, are by Yoshikawa and Suto [14]. The transformation temperature decreases with increasing MgO concentration both on heating and cooling. The dependence of the MgO concentration midpoint between the transformation temperatures on heating and cooling is given by $\Delta TT/\Delta C = -67\,\mathrm{K\,mol\%}$ MgO, where TT is the transformation temperature midpoint and C the concentration of MgO. Yoshikawa and Suto [14] reported $\Delta TT/\Delta C = -370\,\mathrm{K\,mol\%}$ Y_2O_3 for ZrO_2–Y_2O_3 alloys containing 0–2 mol% Y_2O_3. This suggests that the stabilization potential of ZrO_2 is much smaller for MgO than for Y_2O_3.

As described in the previous section, the diffusion of Mg ions in the ZrO_2 lattice for decomposition takes place substantially at high temperatures above 1320 K, where the t-phase is in a metastable condition as can be seen from Fig. 12. This suggests that the product of eutectoid decomposition, Equation 2, is the t-phase and not the m-phase. Because the decomposition reactions proceed consuming the original c- and t-phases containing 9.7 mol% MgO, the increase of the high-temperature stage results in the decrease of the low-temperature stage.

The high-temperature stage shifts to higher temperatures with increasing number of cycles. There are two possibilities causing the temperature shift, one of which is the production of microcracks and the other is the further decrease of MgO concentration in the matrix. Once produced, the microcracks provide preferable sites for the volume-increase transformation, such as the t- to m-phase transformation in the next cycle, and make the m-phase more stable. This shifts the high-temperature stage to higher temperatures. If the concentration of MgO in the matrix decreases further towards zero, as expected from the phase diagram shown in Fig. 12, after decomposition into low-MgO-content t- or m-phase matrix and MgO particles, the transformation temperature shifts to higher temperatures up to the transformation temperature of pure ZrO_2. The concentration of MgO in the matrix is 1–2 mol% after 68 cycles. However, the mean diffusion distance of Mg ions is evaluated to be only 4.0×10^{-1} μm even for 68 cycles. Although further cyclic experiments or prolonged ageing treatments will be needed, it is likely that the equilibrium composition has not been reached in the present experimental conditions and that the concentration of MgO in the matrix decreases further.

5. Conclusions

1. The oblate ellipsoidal t-phase precipitates, 20–50 nm in diameter and 100–200 nm long, in the as-sintered specimen were below a critical size for transformation and exhibited no transformation in the first three cycles.

2. In the fourth and further cycles, the t–m transformation occurred in two distinct stages. A low-temperature stage appeared at 850–1000 K on heating and at 400–700 K on cooling, while the high-temperature stage appeared at 1350–1400 K on heating and at 1000–1200 K on cooling. The low-temperature stage was dominant in the low range below ten cycles, while the high-temperature stage was dominant in the high range above 20 cycles.

3. During cyclic heating and cooling, coarsening of the oblate ellipsoidal precipitates and decomposition of the c- and t-phases into MgO and a low-MgO-content m- or t-phase occurred. Repeated transformation produced a large number of microcracks mainly along grain boundaries.

4. It is concluded that the low-temperature stage was caused by martensitic transformation of the coarsened ellipsoidal precipitates of t- and m-phases, containing 9.7 mol% MgO, in the c-phase matrix. The high-temperature stage was caused by martensitic transformation of the low-MgO-content m- and t-phases containing 1–2 mol% MgO produced by the decomposition.

Appendix

The solution of Equation 4 can be expressed [16, 17] with the aid of the exponential integral

$$Ei(-x) = \int_{-\infty}^{-x} [\exp(x)/x] \qquad \text{(A1)}$$

Equation 4 then becomes

$$X_n = (2nD_0/\alpha)^{1/2}\left\{\left[\int_0^{T_{max}} \exp(-Q/RT)\,dT\right]^{1/2} - \int_0^{T_{min}} \exp(-Q/RT)\,dT\right]^{1/2}\Bigg\}$$
$$= (2nD_0 Q/\alpha R)^{1/2}\{[(RT_{max}/Q)\exp(-Q/RT_{max}) + Ei(-Q/RT_{max})]^{1/2} - [(RT_{min}/Q)\exp(-Q/RT_{min}) + Ei(-Q/RT_{min})]^{1/2}\} \quad (A2)$$

In the present temperature range between room temperature and 1490 K, one can set

$$Q/RT \gg 1$$

for $Q = 239\,\mathrm{kJ\,mol^{-1}}$ [11] for Mg ions in the ZrO_2 lattice, and the exponential integral can be approximated as

$$Ei(-Q/RT) \doteqdot \exp(-Q/RT)\,[(RT/Q)^2 - (RT/Q)] \quad (A3)$$

Using Equation A3, finally we obtain

$$X_n \doteqdot (2nR/\alpha Q)^{1/2}\,(T_{max}\,D_{max}^{1/2} - T_{min}\,D_{min}^{1/2}) \quad (A4)$$

where $D_{max} = D_0 \exp(-Q/RT_{max})$ and D_{min} $D_0 \exp(-Q/RT_{min})$.

References

1. D. J. GREEN, R. H. J. HANNINK and M. V. SWAIN, "Transformation toughening of ceramics" (CRC Press, Boca Raton, FL, 1989) pp. 1–197.
2. C. F. GRAIN, *J. Amer. Ceram. Soc.* **50** (1967) 288.
3. D. L. PORTER and A. H. HEUER, *ibid.* **62** (1979) 298.
4. R. H. J. HANNINK, *J. Mater. Sci.* **18** (1983) 457.
5. B. C. MUDDLE and R. H. J. HANNINK, *J. Amer. Ceram. Soc.* **69** (1986) 547.
6. R. R. HUGHAN and R. H. J. HANNINK, *ibid.* **69** (1986) 556.
7. S. C. FARMER, A. H. HEUER and R. H. J. HANNINK, *ibid.* **70** (1987) 431.
8. R. H. J. HANNINK, *Mater. Forum* **11** (1988) 43.
9. R. H. J. HANNINK and M. V. SWAIN, in "Tailoring of multiphase and composite ceramics conference", edited by G. L. Messing, C. G. Pantano and R. E. Newnham (Plenum Press, New York, 1986) pp. 259–79.
10. U. DWORAK, H. OLAPINSKI and W. BURGER, *J. Amer. Ceram. Soc.* **69** (1986) 578.
11. Y. SAKKA, Y. OISHI and K. ANDO, *Bull. Chem. Soc. Jpn* **55** (1982) 420.
12. V. S. STUBICAN and S. P. RAY, *J. Amer. Ceram. Soc.* **60** (1977) 534.
13. W. D. KINGERY, H. K. BOWEN and D. R. UHLMANN, "Introduction to ceramics" (Wiley, New York, 1976) pp. 583–645.
14. N. YOSHIKAWA and H. SUTO, *J. Jpn. Inst. Metals* **50** (1986) 108.
15. R. H. J. HANNINK, *J. Mater. Sci.* **13** (1978) 2487.
16. W. E. PARKINS, G. J. DIENES and F. W. BROWN, *J. Appl. Phys.* **22** (1951) 1012.
17. A. C. DAMASK and G. J. DIENES, "Point defects in metals" (Gordon & Breach, New York, 1971) pp. 145–61.

Received 30 August 1995
and accepted 17 July 1996